

International Advanced Research Journal in Science, Engineering and Technology
Impact Factor 8.311

Refereed journal

Vol. 12, Issue 11, November 2025

DOI: 10.17148/IARJSET.2025.121111

Research on the Reconstruction of Computer-Aided Design (CAD) and Computed Tomography (RP) Models from CT Data

Abdulmuhssin Binhssan

Security Forces Hospital, Riyadh, Saudi Arabia

Abstract: The use of computed tomography (CT) scans enables physicians to diagnose patients without relying solely on anatomy to identify injuries. Instead, they can directly understand the cause of disease through these scans. Since CT scans are simply a series of two-dimensional images, this study aims to reconstruct a three-dimensional holographic model from these CT scans to provide medical staff with a reference for judgment and diagnosis. This increases diagnostic accuracy and ease of use, and enables physicians to better understand injuries.

This study relies on a series of CT scans and computer-aided design (CAD) of B-spline curves and surfaces. Using MATLAB, a program was developed to reconstruct three-dimensional models from the CT scans. This allows users to visualize the reconstructed three-dimensional model of the CT scans and then export it from a rapid prototyping device as a holographic model. This study uses an example to create an artificial hip model for demonstration and observation. Furthermore, the completed three-dimensional model is available online to explore the feasibility of virtual surgery. This research aims to shorten the duration of surgical training for trainees by enabling mesh surgery.

Keywords: Computed tomography, computer-aided design, B-spline curves and surfaces, 3D reconstruction, rapid prototyping, virtual surgery.

1. Introduction

Reverse engineering (RE) in computer-aided design (CAD) has seen significant growth in recent years. Its basic construction method is to convert raw point cloud data into a model using a reverse engineering or computer-aided design (CAD) system. This process is generally considered a traditional reverse engineering technique. The benefits of this technique not only save craftsmen and engineers time in creating and improving the model, but it also shortens discussions between the client and the manufacturer. If the designer is not satisfied with the final product, a new model can be created with minimal computer modification. This method is considered more convenient and time-saving in product development compared to traditional advanced engineering in computer-aided design (CAD). Reverse engineering has also become widely used in medical imaging. Visualization of medical images, ranging from early Xrays to more recent computed tomography (CT) and magnetic resonance imaging (MRI), can be achieved through reverse engineering. This differs from traditional reverse engineering techniques and is referred to as non-traditional reverse engineering (RE) (see Table 1). However, since X-ray, CT, and MRI images are single-layer, two-dimensional images, physicians must analyze these layers one by one during diagnosis. Using this sequence of layers to mentally determine the spatial location of a lesion requires considerable imagination and expertise. Therefore, converting these images into three-dimensional models through reverse engineering techniques to provide a reference for medical diagnosis is a research direction worth exploring. Generally, a 3D computer model reconstructed using CAD is used to generate a three-dimensional solid model through rapid prototyping. After the 3D computer model is combined with a rapid prototyping machine, it can also directly output solid organ models, such as artificial ears, artificial hearts, artificial joints, skull patches, prosthetic limbs, etc. [1][26]. For human organs with few discrepancies, this has significant application value. Furthermore, CAD and RP-based CT processing technology can be used for the manufacture of artificial organs, medical demonstration, or teaching. In addition, online virtual reality technology can also be applied to develop and create a virtual surgical system as a reference for planning surgical guidance or surgical trajectory, thus achieving the full application of medical imaging.

2. REVIEW OF RELATED LITERATURE

Non-contact endoscopic scans (X-rays, CT, and MRI) are widely used in computer-assisted surgery (CAS). With the help of 3D imaging, 3D images can be used for preoperative training to determine the best surgical approaches and



International Advanced Research Journal in Science, Engineering and Technology Impact Factor 8.311 Refereed journal Vol. 12, Issue 11, November 2025

DOI: 10.17148/IARJSET.2025.121111

trajectories. During surgery, 3D images, combined with robotic arms, guide the surgeon to the correct surgical site. 3D imaging assessments can then be performed postoperatively.

		Traditional reverse engineering		Non-traditional reverse engineering	
Original Model	Original Model	Hard model Soft model	Hard model	human organs	Rubbings of inscriptions Calligraphy and paintings
Hardware Equipment and Pre- processing	Measurement platforms	lasers	Scanners, 3D measuring instruments	(CT, MRI) scanners	medical measuring instruments
	Pre-treatment technology	Model surface smoothing (model filling, surface finishing, etc.)		No special pre-processing required	
Data Format Processing	File format conversion	Generally, in ASCII file format		Convert grayscale image files into point cloud data (image edge detection, coordinate data conversion, etc.)	
	Data size	Determined by the size of the measurement interval		Determined by the size of the image feature	
	Data fitting pattern	3D Free Curve		2D contour curve	
Model Construction	3D model construction	Constructed from characteristic curves and edge curves		Created by sweep-blending the contours of each layer.	

Table 1: Differences between traditional and non-traditional reverse engineering techniques

Medical imaging research, primarily focusing on non-contact endoscopic scans, has been widely discussed in academic circles in recent years. In discussing the relevant literature, it can be roughly divided into four aspects: (1) medical image processing [3][8][15][18][23][24] (2) medical image reconstruction based on curves and surfaces [2][7][20][21] (3) rapid manufacturing of medical prosthetic organ models [4][27] (4) retinal virtual medical image reconstruction and virtual surgery system [12][22]. At present, domestic and foreign universities in medical engineering, information engineering, engineering, mechanical engineering, electrical engineering, industrial design, etc., and teaching hospitals have partially combined or integrated the above four aspects as research directions. In related research, a comprehensive review is made here; Lin Zhiyong [1] combined image segmentation and edge detection technology for image processing with surface fitting for reverse engineering to reconstruct 2D medical engineering models into 3D stereoscopic models. Guo Taihong [4] combined and created a set of medical imaging development software primarily used in oral and maxillofacial surgery, combining it with RP to produce metal bone plates or implants, thus improving surgical precision and reducing surgical time. Liu Minghui [12] discussed a method for constructing interpolation data between CT images, combining linear interpolation and shape interpolation methods to create new layers based on speed and accuracy. Guo [19] used deformation theory as a basis for performing interpolation operations on 3D medical images to directly segment 3D grayscale volume data. Otsu [25] mentioned the use of statistical methods to select the critical value of an image.

Regarding geometric model construction, Anand [14], Choi [17], and Watt [29] provided a comprehensive introduction to common curve and surface construction patterns in the CAD/CAM field and compared the characteristics of different curve and surface constructions. Tsai [28] directly explored the cross-sectional contours of medical images and used geometric models to complete the layer-to-layer flattening application. Liu Guangyun [9] used a gradient image approximation algorithm to create a system that can simultaneously monitor and reconstruct 2D and 3D spinal images to improve clinical spine surgery (commonly known as bone spur removal) without the hassle of external markers, thus increasing surgical accuracy. Li Wusong [10] used craniofacial plastic surgery as a guide, used CT image files, and reconstructed implant models through image processing and computer graphics techniques. He then used a rapid prototyping machine to produce a physical object and completed the production of a silicone master model to provide a bone gap for clinical implant injuries. Jian Jianzhi [11] explored the integration of CT and MRI images of the brain, reconstructing a 3D head image by retaining the clear skull image of the CT scan and the characteristic grayscale brain tissue image of the MRI scan, and establishing a surgical guidance system for precise surgical positioning.



Impact Factor 8.311

Refereed journal

Vol. 12, Issue 11, November 2025

DOI: 10.17148/IARJSET.2025.121111

3. RESEARCH METHODOLOGY

This research paper primarily explores the use of geometric features to reconstruct point sets between contour lines in medical images. A 3D medical image reconstruction system was developed through the development of a Matlab application program. This system automatically reconstructs 3D CAD models from 2D CT images. The system then generates physical 3D medical prototypes using a rapid prototyping machine. These prototypes can be viewed online, improving the readability of medical image files. This research paper first processes the CT scan files. The main steps involve the use of image processing techniques to identify the target contour line. The coordinates of the resulting points are randomly ordered according to the contour line shape. Characteristic control points for the contour line are then derived. Using patching within the curved surface method, the overlapping contour points are patched to reconstruct a 3D surface structure. The developed system includes user-controllable features, allowing the reconstructed model to be freely scaled and rotated within the window, enabling users to view and evaluate it from any angle. Another line of research is the integration of reconstructed 3D medical images with virtual reality systems, allowing them to be viewed directly through a browser or used in surgical simulations and training, thereby reducing damage to surrounding tissue during future surgeries. For rapid prototyping applications, the reconstructed model can be converted to an STL file using the CAD conversion software Solid View, allowing a 3D model to be generated from a rapid prototyping device. The figure illustrates the structural flowchart of this study.

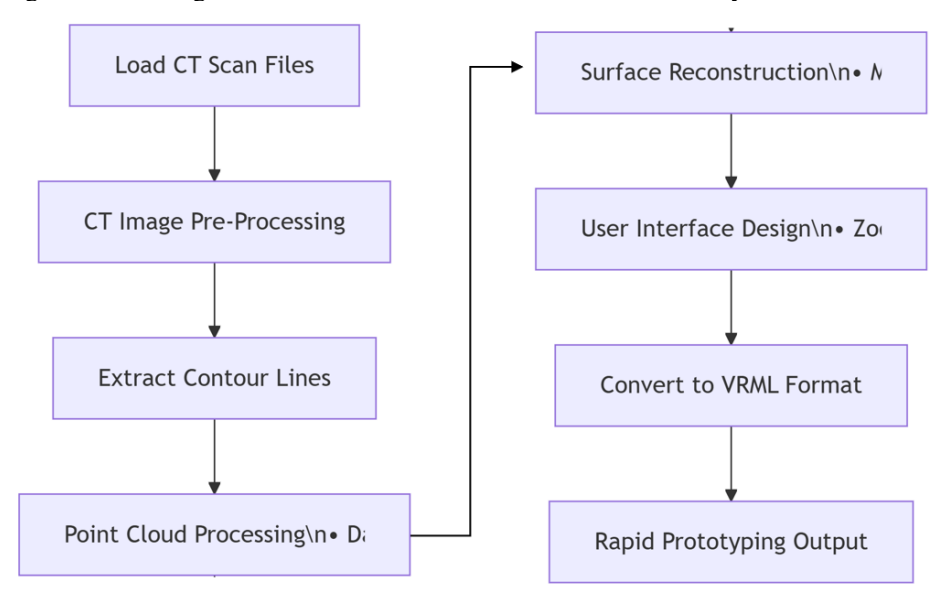


Fig.1 System Architecture

The detailed steps are as follows:

1. Use median filtering rules for image processing techniques [25] to filter out noise in the image. 2. Use image processing techniques to find the appropriate critical value [5]. 3. Convert the image to binary format to find the desired tissue structure. 4. Find and visualize the contour boundaries. 5. Create contour lines in different colors with the original image to check for unreasonable areas. 6. Adjust the adjacent contour point sets according to the curved surface. 7. Reconstruct the 3D surface model and add visual elements (light source, reflection coefficient, etc.). 8. Complete a 3D reconstruction system for the CT scan [30]. 9. Convert the resulting graphics to a virtual reality file format that can be viewed directly in a browser. 10. Convert the WRL format to STL format and then generate an RP file as a 3D model for display and verification.

4. CT IMAGE CAPTURE

CT image capture primarily relies on the use of image processing techniques to determine the desired image contour. The resulting point coordinates are randomly arranged according to the shape of the contour. Characteristic control points of the contour are then derived. Spline surfaces, a geometric method for characterization, are then used to connect sets of contour points and reconstruct a 3D surface structure. Figure 2 illustrates the CT image acquisition process for this study.

4.1 Histogram.

A histogram is a statistical graph showing the distribution of grayscale values across all pixels in an image. For an 8-bit grayscale digital image, the horizontal axis typically represents 256 grayscale pixel values (2 to the eighth power, from



DOI: 10.17148/IARJSET.2025.121111

0 to 255), while the vertical axis represents the cumulative number of pixels with that grayscale value. For example, as shown in Figure 3, a histogram with a horizontal axis (grayscale value) of 100 and a corresponding vertical axis of 520 indicates that there are 520 pixels with a grayscale value of 100 in the image. Therefore, the area of a histogram represents the total number of pixels in an image. If the pixel area occupied by a given grayscale value is divided by the total area, it represents not only the proportion of those pixels but also the probability of that value appearing in the image. Histograms are commonly used to determine and understand the distribution of brightness and darkness in an image. If an image is too dark and unclear, the histogram can be adjusted using statistical correlation calculations to achieve a level of clarity suitable for the naked eye. This type of operation, called histogram equalization, compensates for human insensitivity to changes in low grayscale images.

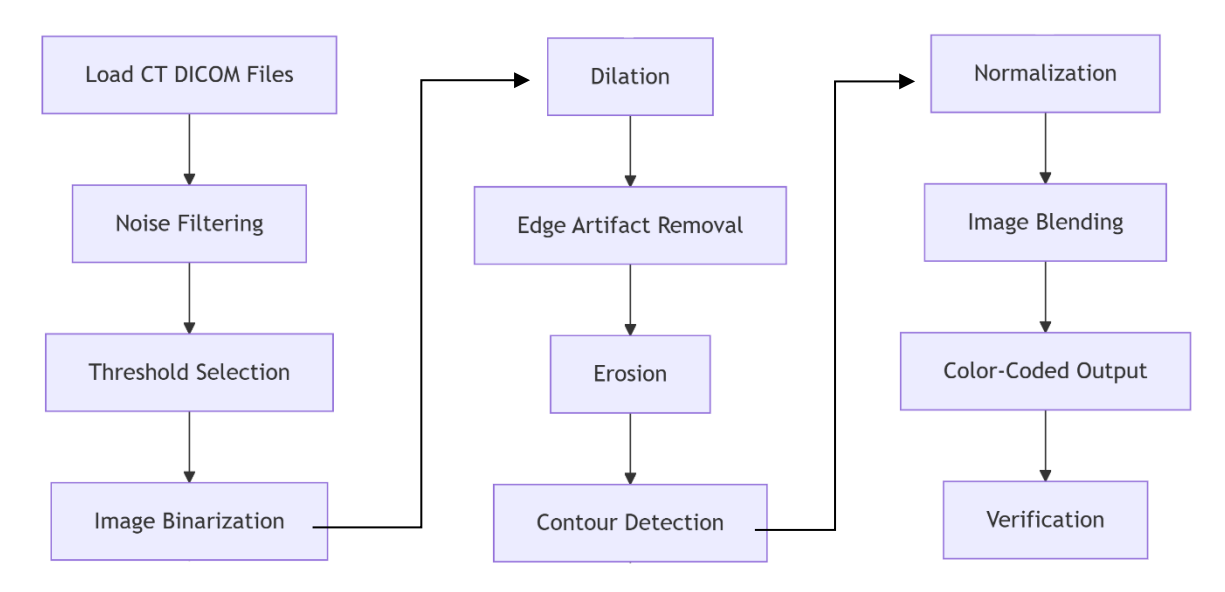


Fig.2 CT image processing flow chart in this article

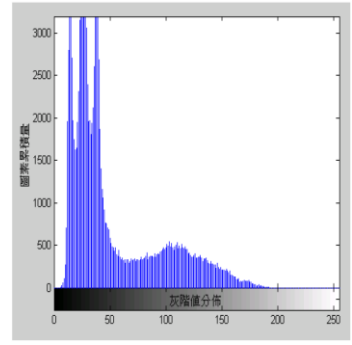


Fig.3 Histogram diagram

4.2 Choosing a Critical Value

The critical value (also known as the threshold, cutoff value, or threshold) is another of the histogram functions mentioned above. Choosing one or more critical values for an image significantly impacts subsequent image processing. Using a single grayscale value as a threshold is also called binary partitioning. This involves choosing an appropriate value to divide the image's histograms. If the image has two distinct peaks, this indicates better foreground and background quality. The threshold value is usually chosen as the grayscale value corresponding to the valley between the two peaks, which represents the critical value.

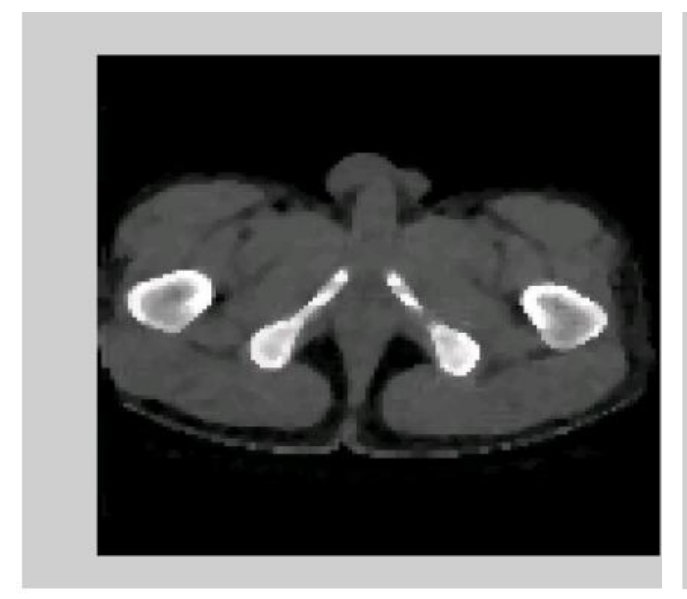
In engineering applications, a threshold value is often used to separate an image into two parts: the background and the foreground. The foreground is usually the desired target, and the background is usually removed. After the foreground is removed, this part is post-processed. For example, a hand-drawn engineering drawing is scanned and saved as a digital file using a CCD camera or scanner. A histogram is calculated. Generally, the distribution of the histogram shows that the foreground and background, i.e., the underlined part and the paper part, are clearly divided into two



Impact Factor 8.311 ເຂົ້າ Peer-reviewed & Refereed journal ເຂົ້າ Vol. 12, Issue 11, November 2025

DOI: 10.17148/IARJSET.2025.121111

regions, i.e., two groups. After taking the threshold value for the binary, the region of interest, i.e., the underlined part, can be clearly extracted for post-processing. The choice of threshold value has a major impact on image post-processing. Domestic and foreign researchers have conducted many studies on threshold value selection, such as the threshold value selection theory proposed by Otsu [25], the dynamic preservation threshold value method, or the fuzzy nerve law for threshold value selection. This study uses Otsu's threshold theory to perform threshold calculations on an image. Figure 4 shows the original image before deconvolution using Otsu's threshold selection method, while Figure 5 shows the image after deconvolution using Otsu's threshold selection method.



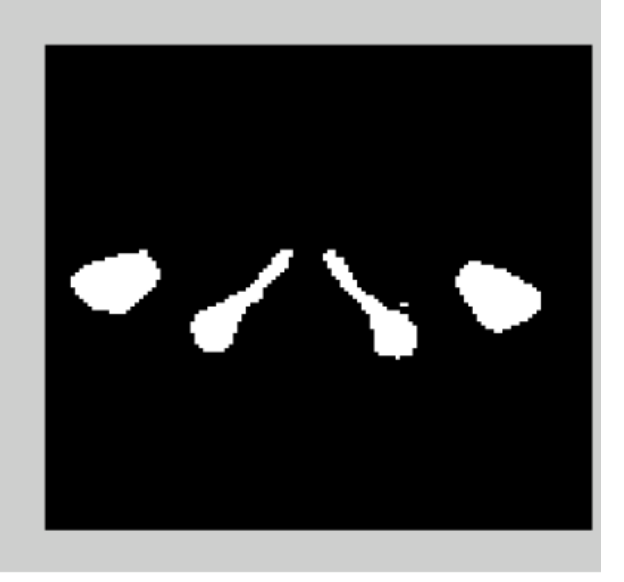


Fig.4 Image without critical segmentation

Fig.5 Image with critical segmentation

4.3 Critical Value Segmentation

Critical value segmentation is the process of segmenting image regions based on the grayscale values of each pixel in the image. Critical value segmentation is generally divided into two methods: single-critical value segmentation and multi-critical value segmentation. A single-critical value segmentation is represented by a unique cluster (R1) for pixels greater than or equal to the critical value (denoted by T), and each pixel less than the critical value is represented by another cluster (denoted by R2). Each cluster is called a segment.

F(x,y) represents the grayscale value of a pixel at coordinates x,y in the image.

R1 =
$$\{(x, y) \mid f(x, y) \ge T\}$$
....(1)
R2 = $\{(x, y) \mid f(x, y) \le T\}$(2)

Multi-critical value segmentation is to give two or more critical values to determine the segmentation area. If two critical values (T1 and T2) are taken as an example, three clusters (denoted by R1, R2, and R3 respectively) can be determined. The mathematical expression is as follows:

The above two types of segmentation, single threshold value segmentation and multi-threshold value segmentation, are global segmentation, which takes the entire image into consideration for calculation.

4.4.1 The Stretching Process

After processing with the structuring element, the gaps are filled and the object's shape is increased. The conditions for this process are divided into the following two steps:

1. When the center of the structuring element moves to a zero point on the image, the structuring element is deactivated and moved down.



Impact Factor 8.311

Refereed journal

Vol. 12, Issue 11, November 2025

DOI: 10.17148/IARJSET.2025.121111

2. When the structuring element moves to a zero point on the image, the four points above, below, left, and right of that point are set to 1, and the process continues downward.

4.4.2 The Smoothing Process

This process is similar to the stretching process, using the same structuring element. After processing with the structuring element, the protrusions are removed, and the object's shape is reduced. The process is divided into the following two steps, in order:

- 1. When the center of the structuring element moves to a zero point on the image, the structuring element is deactivated and moved down.
- 2. When the structuring element moves to a point on the image equal to 1, the values of the four adjacent points (top, bottom, left, and right) are determined and set to 1. The point is then moved downward. If all four adjacent values are equal to 1 simultaneously, the point is set to 1. If none of them are equal to 0 simultaneously, the point is set to 0 and moved down one point.

4.4.3 Opening and Closing

Opening and closing are two common operations in image processing. They are simply two different operations, in the order of erosion and dilation. Opening is performed first, followed by dilation, and its purpose is typically to smooth contour lines, cut narrow lines, or remove thin branches. Dilation followed by shrinkage is called closing, and its purpose is to connect narrow discontinuities and long, thin areas around or within the image, remove small internal gaps, and fill in gaps in contour lines. After performing a discontinuity operation on an image, its graphical properties change: noise disappears, the structure softens, and surrounding ridges are removed. This operation is well suited for de-burring tools. However, the closure process can fill or stabilize small internal holes using the expansion process, and then restore the original shape using the shrinkage process, making it ideal for finding contour lines.

4.4.4 Labeling

Labeling is the process of registering different, independent objects in an image by labeling them with different label values. This allows for independent, categorized processing of regions of interest in post-processing, rather than processing the entire image.

4.5 Generating Grayscale Volume Data

Grayscale volume data generation relies on using pre-convolutional tissue images to generate grayscale values for unknown layers between layers using interpolation. Convolution is not performed initially to preserve the complete grayscale data within the solid region. The combination of the input layer and the original layer can be visualized as a three-dimensional matrix. Each element in the matrix represents a single voxel of solid image data within the entity. The grayscale value corresponding to the corresponding position in the upper and lower cross-sections is determined by the grayscale value of the corresponding position. Grayscale volume data are typically derived from a series of connected 2D tomographic images. However, due to practical limitations, the actual distance between two adjacent images is often greater than the unit thickness of the volume. This means that these tomographic images are captured at a constant sampling rate within the observed tissue. Therefore, the required volume data cannot be derived directly from the set of these connected images. Interpolation is used to fill in the missing grayscale data between the original layers. For tomographic images, the mapping method used consists of directly using the top and bottom points of the image, with identical 2D coordinates, as the reference and target points. The insertion point of the line joining the two points is determined using a linear interpolation method, and the formula used is as follows:

M is the number of interpolation layers.

- (,) R I x y is the grayscale data in the reference image.
- (,) T I x y is the grayscale data in the target image.
- (,) m I x y is the grayscale data corresponding to the X and Y coordinates of the MTh layer position.

5. CONSTRUCTION OF CT GEOMETRIC MODEL

There are many methods for creating free curves and surfaces in CAD systems, among which B-Spline curves are the most common. B-Spline curves and surfaces originated in 1972 and were proposed by Cox and de Boor as a new



Impact Factor 8.311

Refered journal

Vol. 12, Issue 11, November 2025

DOI: 10.17148/IARJSET.2025.121111

method for constructing curves and surfaces [17][29]. This study uses B-Spline curves and surfaces to calculate the contour lines of CT.

5.1 B-Spline curves

The construction of curves and surfaces is to control the shape of the curves and surfaces by using a group of control points. When the curve is a composite curve, if a control point is changed in the B-Spline curve, the curve will only change locally and will not have a significant impact on the shape of the curve. In addition, at the connection points of the line segments, its first-order and second-order derivatives will automatically meet the continuity conditions. For a general uniform cubic B-Spline curve, the basis function N is the same across all equally divided segments. The general formula is as follows:

-(--)---(--)I NID (7)

r(u)=r(u)UNR.....(7)

When two B-Spline curves are joined, the following conditions must be met to ensure C2 (curvature) continuity:

ra(u)=rb(u)UNRa.....(8)

rb(u)=rb(u)UNRb.....(8)

5.2 B-Spline Surface Fitting

In this paper, surface fitting is performed using a patching method. When two surfaces are extended along the u and v directions, the curve at the junction of the two surfaces can be joined to satisfy C2 (curvature) continuity to calculate the next surface. Figure 7 shows a patching method written in Matlab for surface fitting along the u direction.

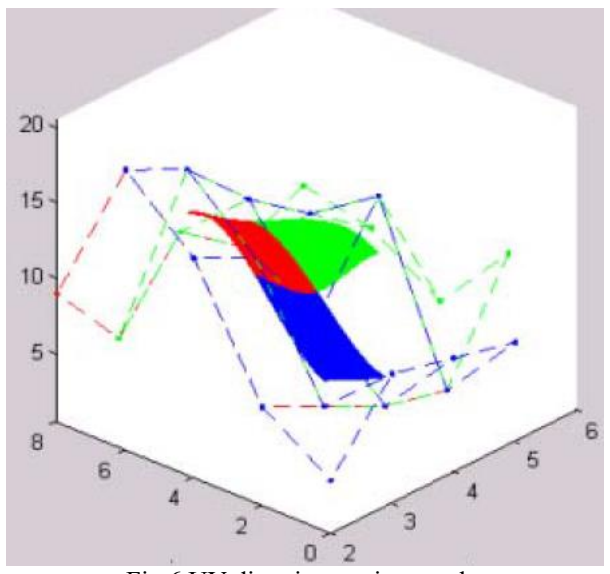


Fig.6 UV direction paving results

Furthermore, assuming the fault map has four layers, the patch generation method in the figure uses 16 control points to create a small patch. In this figure, these are organized into seven groups of control points, or seven groups of control surfaces, thus generating seven patches. The patches fit together to create the image shown in Figure 8. Figure 9 shows the patching process continuing in the vertical direction following Figure 8.



International Advanced Research Journal in Science, Engineering and Technology Impact Factor 8.311 Refereed journal Vol. 12, Issue 11, November 2025

DOI: 10.17148/IARJSET.2025.121111

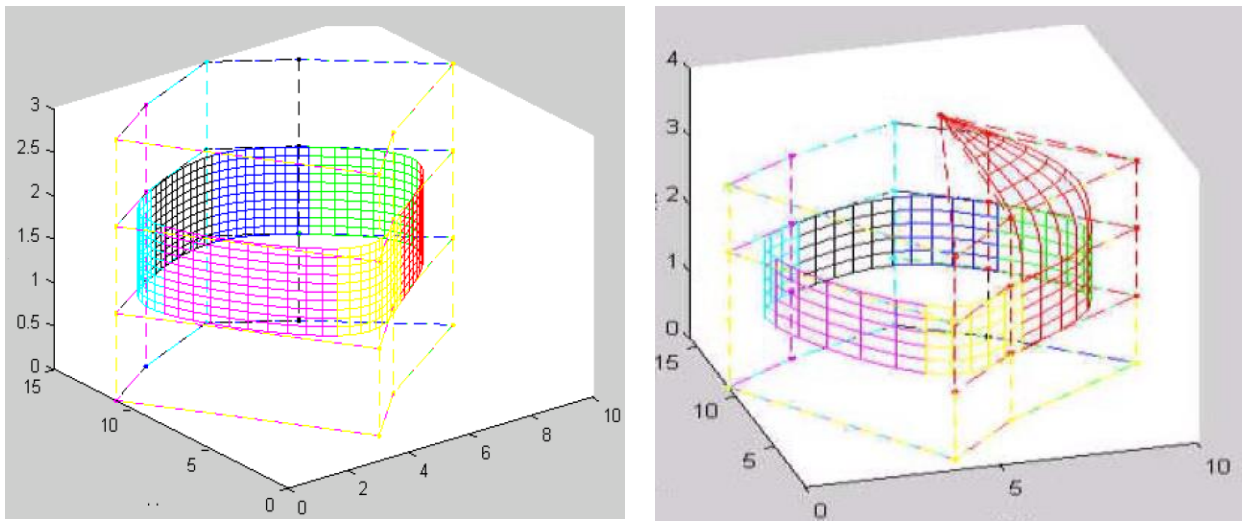


Fig.7 Patches pavement situation in space

Fig.8 Longitudinal Pavement Results VI.

6. EXAMPLE VERIFICATION

In this study, the 3D reconstruction example used a hip CT image (a CT image provided by 3D Doctor for testing). The main steps involved extracting the relevant region from the contour and reconstructing a set of 3D contour points from these regions. The contour extraction steps are as follows: reading the image file, performing image enhancement, selecting a filter to filter out noise, finding a suitable threshold for binary, performing image expansion and contraction, and performing a logical operation to extract the contour. The contour points are displayed in different colors and compared to the original CT image to identify inappropriate regions. The contours are sorted, and a linear curve is drawn. Finally, a 3D surface is constructed based on the feature control points and the linear curve.

6.1 3D Reconstruction of Hip CT Images

To process a single hip image, a complete contour extraction program can be developed in Matlab. To facilitate comparison of results, the results are displayed with a red outline next to the original image. Figure 10 illustrates the processing steps for hip.



Fig.9 Image processing of the 41st slice of the hip CT scan



Impact Factor 8.311

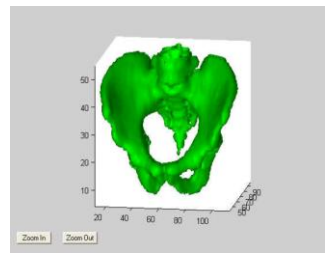
Reer-reviewed & Refereed journal

Vol. 12, Issue 11, November 2025

DOI: 10.17148/IARJSET.2025.121111

6.2 Hip 3D Reconstruction

After determining the coordinates of the hip contour points, the contour points can be laid out using MATLAB. For easier observation and aesthetic presentation, conventional visualization functions such as scaling, rotation, and different viewing angles are also implemented. Lighting and reflection coefficients are also added to complete the 3D CAD model of the hip, as shown in Figures 11 and 12.



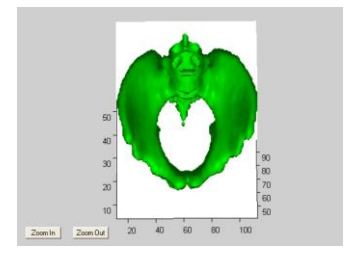


Figure 10 Hip Bone 3D Reconstruction Results (Top View)

Figure 11 Hip Bone 3D Reconstruction (Isometric View)

The reconstructed 3D model can be exported in Virtual Reality Modelling Language (VRML) format, allowing direct viewing on various browsers, such as Internet Explorer. Using Solid View, the CAD file exchange software, the VRML model file used in this study can be converted into an STL file acceptable to the RP. This file can then be exported to a 3D printing rapid prototyping machine, resulting in a model for display and verification. Figure 14 shows the hip bone displayed in a browser. Figure 15 shows a scaled-down version of the reconstructed model combined with the rapid prototyping output.

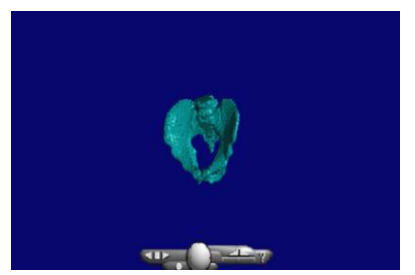


Figure 12 Hip Bone Model Displayed in a Browser



Figure 13 Solid Model Completed Using RP

7. CONCLUSION

The results of this study demonstrate the image processing process and 3D reconstruction results of 2D hip CT scans. The models generated in this study can be reconstructed without using a CAD system, reducing the time and complexity of CAD surface manipulation. The reconstructed 3D surfaces or solid models can also be converted into a virtual reality (WRL) file format for direct viewing and manipulation via an internet browser, allowing users to observe and evaluate the reconstructed 3D CT files. The specific achievements of this study are as follows:

- 1. Automatic extraction of contour point sets from various CT images.
- 2. Completion of 3D feature rendering using internally developed spline chips.
- 3. Direct addition of lighting and reflection parameters, etc., to the finished 3D graphics within the reconstruction system, improving readability and realism.
- 4. Ability to convert finished 3D models to VRML format. 5. VRML files can be converted to STL format, the standard format for rapid prototyping machines.
- 6. Finished models can be exported from rapid prototyping machines for preview and verification.

REFERENCES

- [1]. Lin Zhiyong (2001), "Reconstructing 3D Virtual Human Organ Models Using Reverse Engineering and Image Processing Technology," 1990 National Science Council Special Research Project Results Report, pp. 1-6.
- [2]. Huang Shengjie (2000), "Using Computed Tomography Data to Establish a CAD and RP Interface System," 1990 National Science Council Special Research Project Results Report, pp. 1-5.



DOI: 10.17148/IARJSET.2025.121111

- [3]. Li Jiande (2000), "Research on Intracranial 3D Image Reconstruction and Positioning Counting," 1990 National Science Council Special Research Project Results Report, pp. 1-5.
- [4]. Guo Taihong, Fang Jingjing, and Wang Dongyao (2002), "Medical Imaging Software Development: Basic Interface and 3D Solid Model Reconstruction," 19th Mechanical Engineering Academic Symposium, pp. 823-830.
- [5]. Miao Shaogang (2000), Digital Image Processing Using Matlab, Quanhua Technology Book Co., Ltd.
- [6]. Liu Minghui (1999), Fast Interpolation Method for 3D Medical Image Reconstruction, Master's Thesis, Institute of Information Engineering, Feng Chia University.
- [7]. Tang Yingxi (2002), Research on 3D Reconstruction and Visualization of Medical Images Based on Geometric Features, Master's Thesis, Institute of Automation, Da-Yeh University.
- [8]. Huang Xinxian (2000), Image Segmentation, Reconstruction, and Stereoscopic Visualization: A Case Study of Magnetic Resonance Imaging of the Portal Vein, Master's Thesis, Institute of Industrial Engineering, Da-Yeh University.
- [9]. Liu Guangyun (2000), Research on the Application of Various Medical Imaging Systems in 3D Spinal Reconstruction and Fusion, Master's Thesis, Institute of Information Engineering, National Cheng Kung University.
- [10]. Li Wusong (2000), Design and Fabrication of Implants for Craniofacial Plastic Surgery, Master's Thesis, Graduate School of Mechanical Engineering, National Central University.
- [11]. Jian Jianzhe (2000), Fusion of Head CT and MR Images, Master's Thesis, Graduate School of Mechanical Engineering, National Central University.
- [12]. Huang Dechang (2000), Application of Image Processing and Virtual Reality in Medicine, Master's Thesis, Graduate School of Mechanical Engineering, National Central University.
- [13]. Liu Minghui (1999), "Fast Interpolation Method for 3D Medical Image Reconstruction," Master's Thesis, Institute of Information Engineering, Feng Chia University.
- [14]. Anand, V.B., (1993), "Computer Graphics and Geometric Modeling for Engineers," John Wiley, Chapter 5.
- [15]. Archip, N. et al., (2002), "A Knowledge-Based Approach for Automatic Spinal Cord Detection in CT Images," IEEE Transactions on Medical Imaging, Vol. 21, No. 12, pp. 1504–1516.
- [16]. Choi, S.H., and Kwok, K.T., (2002), "Hierarchical Cutting Contours for Layered Manufacturing," Computers in Industry, Vol. 48, pp. 219–239.
- [17]. Choi, B. K. (1991), Surface Modeling for CAD/CAM, Elsevier, Chapters 3 and 4.
- [18]. David R. Soll (1999), "Computer-Aided Three-Dimensional Reconstruction and Motion Analysis of Living and Crawling Cells," Computer Imaging and Medical Graphics, vol. 23, pp. 3–14.
- [19]. Guo, J. F., Cai, Y. L., and Wang, Y. P. (1995), Morphology-Based Interpolation for 3D Medical Image Reconstruction, Computer Imaging and Medical Graphics, vol. 19, no. 3, pp. 267–279.
- [20]. Lee, T. Y., and Lin, C. H. (2002),
- [21]. "Feature-Guided Shape-Based Image Interpolation," IEEE Transactions on Medical Imaging, vol. 21, No. 12, pp. 1479–1489.
- [22]. Lotjonen, J., et. al., (1999), "3D Geometry Reconstruction Using 2D Profiles and a Geometric Prior," IEEE Transactions on Medical Imaging, vol. 18, no. 10, pp. 992–1002.
- [23]. Marovic, B., Jovanovic, Z., (1998),
- [24]. "Visualization of 3D Fields and Medical Data Using VRML," Future Generation Computer Systems, vol. 14, pp. 33–23. Maksimovic, R., Stankovic, S., and Milovanivie, D. (2000), "Computed Tomography Image Analyzer: 3D Reconstruction and Segmentation Using Active Contour Models 'Snakes'," International Journal of Medical Informatics, pp. 29–37.
- [25]. McInereny, T., and Terzopoulos, D. (1999), "Topology-Adaptive Deformable Surfaces for Medical Image Volume Segmentation," IEEE Transactions on Medical Imaging, vol. 18, no. 10, pp. 840–850.
- [26]. Otsu, N. (1979), "A Method for Threshold Selection from Gray-Level Histograms," IEEE Transaction on Systems, Man, and Cybernetics, vol. SMC-9, no. 1, pp. 62-66.
- [27]. Sanghera, B., et. al., (2001), "A preliminary study of rapid prototyping medical models," Rapid Prototyping Journal, vol. 7, no. 5, pp. 275-284.
- [28]. Swann, S., (1996), "Integration of magnetic resonance imaging and stereolithography to build medical models: A case study," Rapid Prototyping Journal, vol. 2, no. 4, pp. 41-46.
- [29]. Tsai, A., et. al., (2003), "A shape-based approach to medical image segmentation using level sets," IEEE Transactions on Medical Imaging, vol. 22, no. 2, pp. 137-154.
- [30]. Watt, A., (2000), 3D Computer Graphics, 3rd ed., Addison Wesley, chap. 3.
- [31]. Liu, S., Ma, W., (1999), "Three-Dimensional Surface Segmentation from CT Contour Data," Computer-Aided Design, vol. 31, pp. 517–536.